INAUGURAL ARTICLE

NEUROSCIENCE

Auditory cortex interneuron development requires cadherins operating hair-cell mechanoelectrical transduction

Baptiste Libé-Philippot[a,b,c], Vincent Michel[a,b,c], Jacques Boutet de Monvel[a,b,c], Sébastien Le Gal[a,b,c], Typhaine Dupont[a,b,c], Paul Avan[d,e,f], Christine Métin[g,h,i,1], Nicolas Michalski[a,b,c,1], and Christine Petit[a,b,c,j,k,1,2]

[a]Unité de Génétique et Physiologie de l'Audition, Institut Pasteur, 75015 Paris, France; [b]UMRS 1120, INSERM, 75015 Paris, France; [c]Sorbonne Universités, Université Pierre et Marie Curie Paris 06, Complexité du Vivant, 75005 Paris, France; [d]Laboratoire de Biophysique Sensorielle, Université Clermont Auvergne, 63000 Clermont-Ferrand, France; [e]UMR 1107, INSERM, 63000 Clermont-Ferrand, France; [f]Centre Jean Perrin, 63000 Clermont-Ferrand, France; [g]Institut du Fer à Moulin, 75005 Paris, France; [h]UMRS 839, INSERM, 75005 Paris, France; [i]Sorbonne Universités, Université Pierre et Marie Curie Paris 06, 75005 Paris, France; [j]Syndrome de Usher et Autres Atteintes Rétino-Cochléaires, Institut de la Vision, 75012 Paris, France; and [k]Collège de France, 75005 Paris, France

This contribution is part of the special series of Inaugural Articles by members of the National Academy of Sciences elected in 2016.

Contributed by Christine Petit, June 9, 2017 (sent for review March 15, 2017; reviewed by Andrej Kral, Botond Roska, and Shihab A. Shamma)

Many genetic forms of congenital deafness affect the sound reception antenna of cochlear sensory cells, the hair bundle. The resulting sensory deprivation jeopardizes auditory cortex (AC) maturation. Early prosthetic intervention should revive this process. Nevertheless, this view assumes that no intrinsic AC deficits coexist with the cochlear ones, a possibility as yet unexplored. We show here that many GABAergic interneurons, from their generation in the medial ganglionic eminence up to their settlement in the AC, express two cadherin-related (cdhr) proteins, cdhr23 and cdhr15, that form the hair bundle tip links gating the mechanoelectrical transduction channels. Mutant mice lacking either protein showed a major decrease in the number of parvalbumin interneurons specifically in the AC, and displayed audiogenic reflex seizures. *Cdhr15*- and *Cdhr23*-expressing interneuron precursors in *Cdhr23*$^{-/-}$ and *Cdhr15*$^{-/-}$ mouse embryos, respectively, failed to enter the embryonic cortex and were scattered throughout the subpallium, consistent with the cell polarity abnormalities we observed in vitro. In the absence of adhesion G protein-coupled receptor V1 (adgrv1), another hair bundle link protein, the entry of *Cdhr23*- and *Cdhr15*-expressing interneuron precursors into the embryonic cortex was also impaired. Our results demonstrate that a population of newborn interneurons is endowed with specific cdhr proteins necessary for these cells to reach the developing AC. We suggest that an "early adhesion code" targets populations of interneuron precursors to restricted neocortical regions belonging to the same functional area. These findings open up new perspectives for auditory rehabilitation and cortical therapies in patients.

tip links | parvalbumin interneurons | neuronal migration | adhesion code | deafness

The study of inherited forms of deafness in humans has greatly advanced our understanding of the molecular and cellular mechanisms underlying sound processing in the auditory sensory organ, the cochlea (1). Most mouse models for these deafness forms faithfully reproduce the hearing deficits observed in humans. Furthermore, most of the genetic forms of profound congenital deafness studied to date can be accounted for by deficits of the cochlea. Many of these deafness forms result from structural and functional abnormalities of the hair bundle (2), a tuft of microvillus-like apical protrusions, the stereocilia, forming the mechanosensitive antenna of the sensory hair cells (Fig. S1*B*).

Early auditory deprivation, such as auditory deprivation due to congenital profound deafness, has major consequences for the maturation of the central auditory system, including the auditory cortex (AC). AC maturation involves successive sensitive periods of cortical plasticity in which several features, such as the tonotopic organization (sound frequency map) of the AC (3) and the balance between neuronal excitation and inhibition (4), are established under the influence of the acoustic environment (5, 6). This neural plasticity is particularly prominent early in life, shortly after hearing onset, and is jeopardized by the lack of auditory stimulation experienced by children with profound congenital deafness. However, early prosthetic interventions, in which profoundly deaf children are fitted with cochlear implants, restore AC maturation through electrical stimulation of the auditory nerve, as indicated by studies in deaf kittens (7, 8).

Much attention has been focused on the impact of auditory deprivation on AC maturation. However, the possibility that AC intrinsic deficits coexist with peripheral auditory deficits in some genetic forms of deafness has not yet been explored despite the expected impact on rehabilitation of the patients. Such associated central intrinsic deficits would probably be masked by the peripheral deficits. Given the major role played by adhesion proteins in brain development, we addressed this issue by studying mouse models for two genetic forms of profound congenital deafness resulting from mutations of *CDHR23* and *CDHR15*, encoding two cadherin-related (cdhr) transmembrane

Significance

In early-onset genetic forms of deafness, deficits of the auditory sensory organ are sufficient to account for the hearing impairment. However, the possibility that intrinsic deficits of the auditory cortex (AC) coexist with the peripheral deficits is still unexplored. We show, in rodents and primates, that the cadherin-related proteins cdhr23 and cdhr15 are expressed by many interneuron precursors targeted specifically to the AC. A deficiency of either protein results in the failure of these interneuron precursors to enter the embryonic cortex and in abnormally small numbers of parvalbumin interneurons in the AC only. These findings should lead to an improvement of hearing rehabilitation strategies in patients and open up new genetic approaches for studying AC development and function.

Author contributions: C.M., N.M., and C.P. designed research; B.L.-P., V.M., J.B.d.M., S.L.G., T.D., and P.A. performed research; B.L.-P., J.B.d.M., C.M., N.M., and C.P. analyzed data; and B.L.-P., C.M., N.M., and C.P. wrote the paper.

Reviewers: A.K., Hannover Medical School; B.R., Friedrich Miescher Institute; and S.A.S., University of Maryland.

The authors declare no conflict of interest.

Freely available online through the PNAS open access option.

[1]C.M., N.M., and C.P. contributed equally to this work.

[2]To whom correspondence should be addressed. Email: christine.petit@pasteur.fr.

This article contains supporting information online at www.pnas.org/lookup/suppl/doi:10.1073/pnas.1703408114/-/DCSupplemental.

proteins, cdhr23 and cdhr15 (also known as cadherin-23 and protocadherin-15, respectively; Fig. S1 *A* and *B*). Within the hair bundle, cdhr23 and cdhr15, which have unusually long ectodomains (9, 10) (Fig. S1*A*), interact through their two most aminoterminal cadherin repeats to form an overlapped, antiparallel heterodimer (11). They form the tip links (12), fine filaments connecting the tip of a stereocilium to the side of the adjacent taller stereocilium that convey sound-evoked mechanical forces to the mechanoelectrical transduction channels. They also form transient lateral links connecting the stereocilia together, and some of the stereocilia with the kinocilium, during hair bundle morphogenesis (13–15) (Fig. S1*B*). The absence of mechanoelectrical transduction currents in the cochlear hair cells is sufficient to account for the profound deafness of patients lacking either cdhr23 or cdhr15 (12, 16). Our explorations of the expression of cdhr23 and cdhr15 during brain development and of mouse mutants lacking either cdhr protein revealed that both proteins were required for the development of GABAergic interneurons in the AC. The development of these interneurons also required adhesion G protein-coupled receptor V1 (adgrv1; also known as gpr98, vlgr1, or mass1), which forms another type of hair bundle links, the ankle links.

Results

***Cdhr23* and *Cdhr15* Are Expressed in the Medial Ganglionic Eminence-Derived Interneurons of the Developing AC.** We first studied the expression profiles of cdhr23 and cdhr15 in the mouse embryonic telencephalon at the end of corticogenesis, on embryonic day (E) 18.5. Both proteins were detected in the neocortex. Remarkably, immunostaining was restricted to the developing AC (Fig. 1*A*). The mammalian neocortex contains glutamatergic excitatory neurons (85% of all neocortical neurons in rodents) and GABAergic inhibitory interneurons (17, 18). In E18.5 *Nkx2.1*-cre:*Rosa*-tdTomato mice, immunostaining for cdhr23 and cdhr15 in the AC was limited to tdTomato-labeled (tdTomato$^+$) neurons, the GABAergic interneuron precursors that are derived from the *Nkx2.1*-expressing progenitors of the medial ganglionic eminence (MGE) and the preoptic area of the subpallium, the ventral part of the telencephalon (19) (Fig. 1*B*). About one-third of AC tdTomato$^+$ neurons were labeled by anti-cdhr23 or anti-cdhr15 antibodies ($30 \pm 3\%$; $n = 10$ embryos). Almost all of these neurons ($96 \pm 1\%$; $n = 5$ embryos on E18.5) stained for one cdhr protein were also stained for the other (Fig. 1*C*). Immunostaining for cdhr23 and cdhr15 persisted in tdTomato$^+$ interneurons on postnatal day (P) 5 (Fig. 1*D*), but had disappeared by P7 (Fig. S2*A*).

We then examined the expression of *Cdhr23* and *Cdhr15* at earlier stages. Unlike glutamatergic neurons, which are generated in the proliferative ventricular zone of the neocortex and migrate radially to form the future six layers of the cortical plate, neocortical GABAergic interneurons undergo a long migration from their place of birth. They first migrate tangentially within the subpallium; then, within the neocortex to reach their final destination; and, finally, radially to their ultimate cortical layer position (20, 21) (Figs. 1*B* and 2*A*). Cdhr23 and cdhr15 were first detected in the telencephalon on E13.5 in newborn tdTomato$^+$ interneuron precursors derived from the ventral MGE mantle zone (Fig. 2 *A*–*C* and Fig. S2 *B* and *C*), but not in their MKI67-immunoreactive proliferating progenitors (Fig. 2*D*) or in the

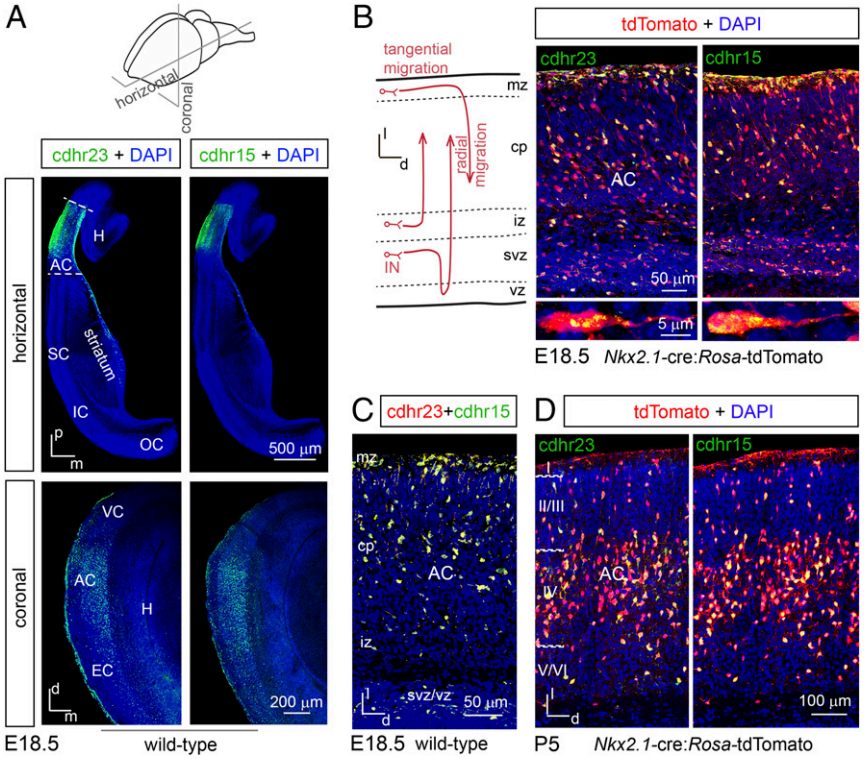

Fig. 1. Expression of *Cdhr23* and *Cdhr15* in MGE-derived interneuron precursors in the developing AC in mice. (*A*) Horizontal (*Upper*) and coronal (*Lower*) sections through the developing AC of wild-type E18.5 mouse embryos immunostained for cdhr23 and cdhr15. (*B*) Diagram of the migration routes of MGE-derived interneurons in the developing neocortex (*Left*), and corresponding coronal sections of the AC of a *Nkx2.1*-cre:*Rosa*-tdTomato E18.5 mouse embryo immunostained for tdTomato and cdhr23 or cdhr15 (*Right Upper*), with detailed views of tdTomato$^+$ cdhr23$^+$, or cdhr15$^+$ interneurons (*Right Lower*). (*C*) Coronal section of the AC of a wild-type E18.5 mouse embryo immunostained for cdhr23 and cdhr15. (*D*) Coronal sections of the AC of a *Nkx2.1*-cre:*Rosa*-tdTomato P5 mouse immunostained for tdTomato and cdhr23 or cdhr15. In the brain horizontal sections of *A* and in *D*, the cdhr23 and cdhr15 immunostainings were carried out on the same sections. Cell nuclei are stained in blue (DAPI). A/S/I/OC, auditory/somatosensory/insular/orbital cortex; cp, cortical plate; d, dorsal; EC, entorhinal cortex; H, hippocampus; IN, interneuron; iz, intermediate zone; l, lateral; m, medial; mz, marginal zone; p, posterior; svz, subventricular zone; VC, visual cortex; vz, ventricular zone.

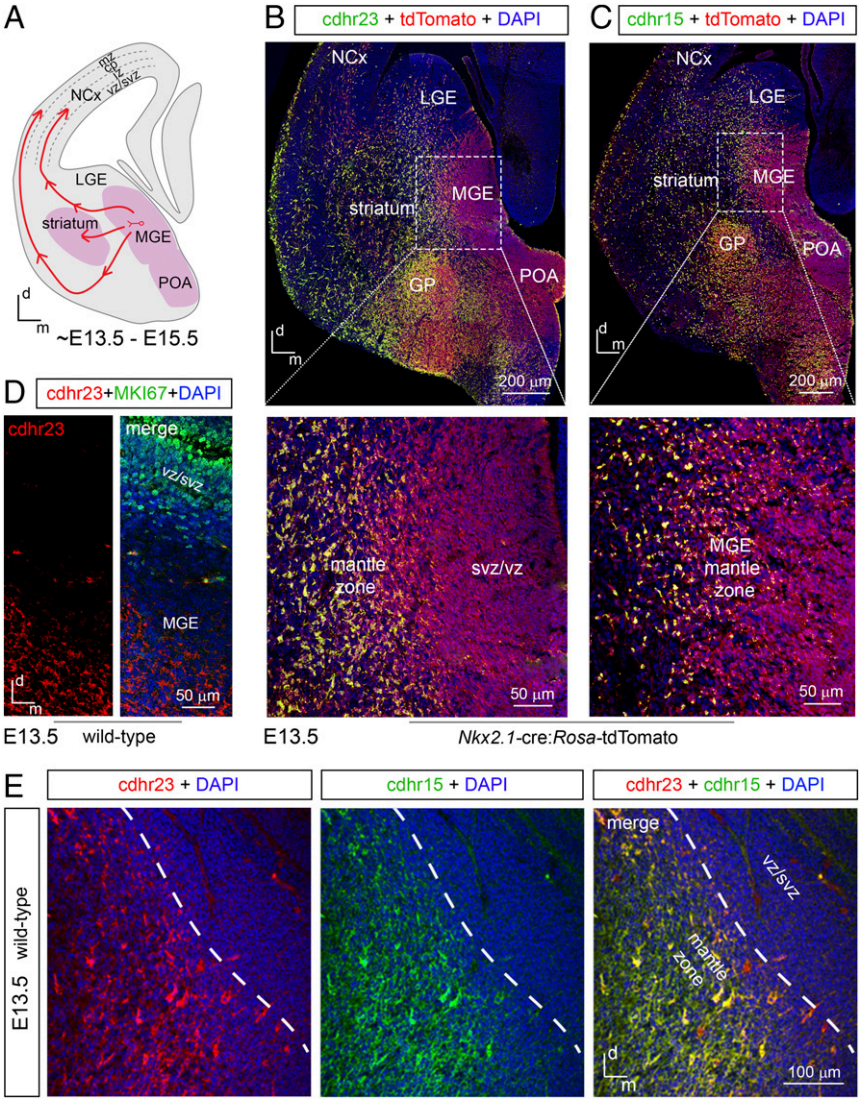

Fig. 2. Coexpression of *Cdhr23* and *Cdhr15* in MGE-derived postmitotic interneuron precursors in mice. (*A*) Diagram of the tangential migration routes of MGE-derived interneurons on a coronal section of the mouse embryonic telencephalon on E13.5–E15.5. Coronal basal telencephalon sections of an *Nkx2.1*-cre:*Rosa*-tdTomato E13.5 embryo immunostained for tdTomato and cdhr23 (*B*, *Upper*) or cdhr15 (*C*, *Upper*) are shown, with detailed views of the MGE shown (*B* and *C*, *Lower*). Note the expression of cdhr23 and cdhr15 in tdTomato$^+$ neurons of the striatum and globus pallidus. (*D*) Coronal sections of the MGE of a wild-type E13.5 embryo immunostained for cdhr23 and MKI67, a cell proliferation marker. (*E*) Detailed view of the MGE of a wild-type E13.5 embryo immunostained for cdhr23 and cdhr15. cp, cortical plate; d, dorsal; GP, globus pallidus; iz, intermediate zone; LGE, lateral ganglionic eminence; m, medial; mz, marginal zone; NCx, neocortex; POA, preoptic area; svz, subventricular zone; vz, ventricular zone.

caudal ganglionic eminence (Fig. S2*D*). Notably, almost all of the neurons of the ventral MGE mantle zone stained for one cdhr protein were also stained for the other (Fig. 2*E*).

Mutant Mice Deficient for *Cdhr23* or *Cdhr15* Have Abnormally Small Numbers of Parvalbumin Interneurons in the AC. We then investigated whether interneurons expressing parvalbumin (PV) or somatostatin (SST) (22), the two GABAergic interneuron populations derived from *Nkx2.1*-expressing progenitors (23, 24), were affected by the absence of cdhr23 or cdhr15. Markedly fewer PV interneurons were detected in the AC of 3-wk-old *Cdhr23*$^{-/-}$ mice (twofold fewer; $P = 0.008$) and *Cdhr15*$^{\text{av-3J/av-3J}}$ mice (4.2-fold fewer; $P = 0.004$) lacking cdhr23 and cdhr15, respectively, than in the AC of their wild-type littermates (Fig. 3*A*). By contrast, the numbers of AC SST interneurons were unchanged ($P = 0.14$ and $P = 0.15$ in *Cdhr23*$^{-/-}$ and *Cdhr15*$^{\text{av-3J/av-3J}}$ mice, respectively; Fig. 3*C*). Despite the strong reduction in the number of PV interneurons in the AC, the cortical thickness of the AC in wild-type (1,007 ± 31 µm, $n = 8$ mice), *Cdhr23*$^{-/-}$ (955 ± 32 µm, $n = 8$ mice), and *Cdhr15*$^{\text{av-3J/av-3J}}$ (980 ± 21 µm, $n = 8$ mice) mice, as well as the estimated surface of the AC per section in wild-type (1.11 ± 0.09 mm^2 per section, $n = 5$ mice), *Cdhr23*$^{-/-}$ (1.16 ± 0.08 mm^2 per section, $n = 5$ mice), and *Cdhr15*$^{\text{av-3J/av-3J}}$ (1.15 ± 0.06 mm^2 per section, $n = 5$ mice) mice, were similar ($P > 0.4$ for all comparisons).

We asked whether this major PV interneuron deficit resulted from the absence of cochlear mechanoelectrical transduction in *Cdhr23*$^{-/-}$ and *Cdhr15*$^{\text{av-3J/av-3J}}$ mice by studying *Cdhr23*$^{+/-}$ and *Cdhr15*$^{+/\text{av-3J}}$ heterozygous mice, which have no cochlear deficit (25) (Fig. S3). At 3 to 4 wk of age, these mice also had fewer PV interneurons in the AC, with interindividual variation, than wild-type mice (1.6-fold and 1.8-fold fewer, on average, respectively; $P < 10^{-3}$; Fig. 3*B*). PV interneuron deficits are often implicated in seizure disorders (26). We therefore investigated the

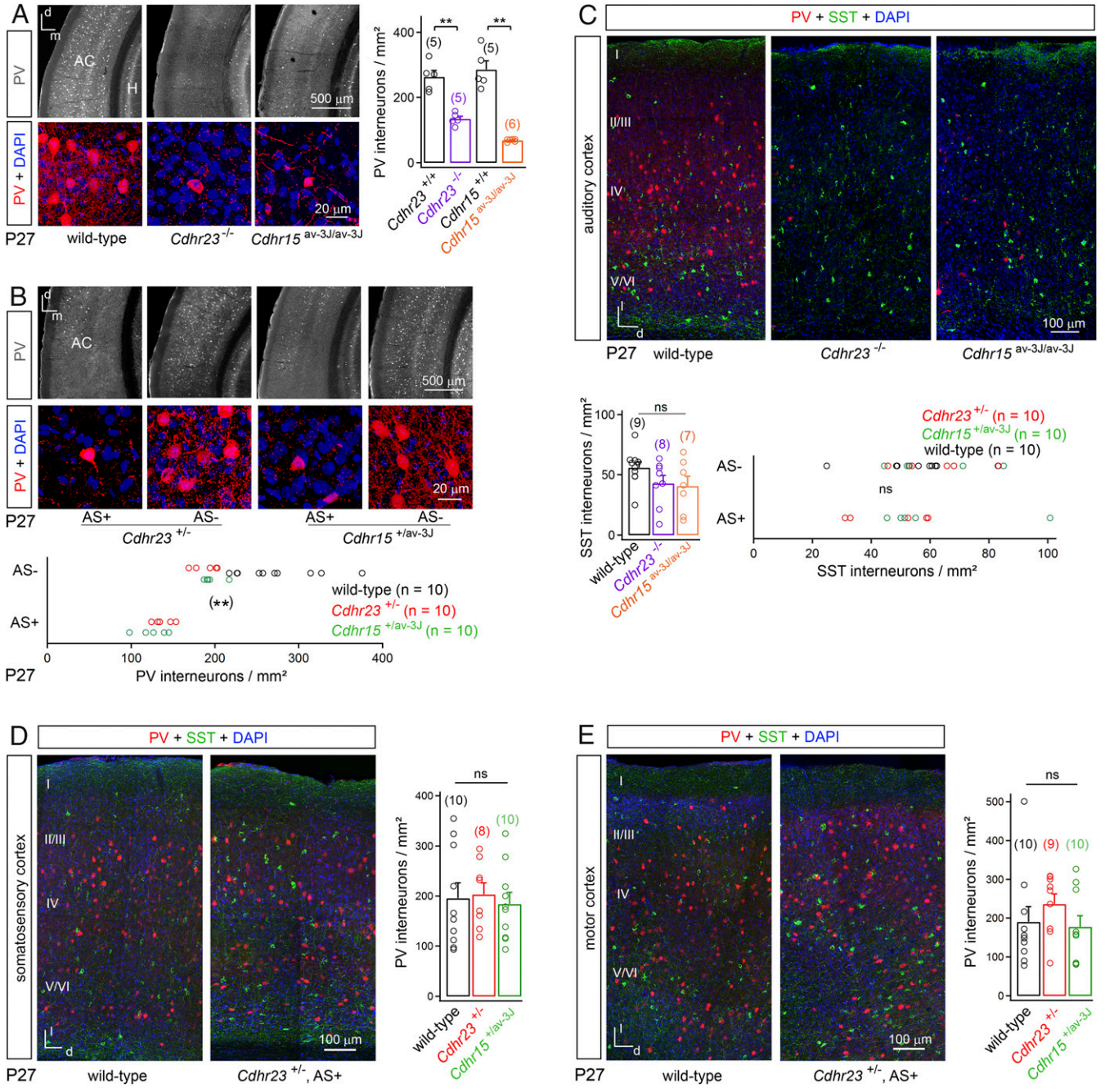

Fig. 3. Abnormally small number of PV interneurons in the AC of mice with mutations of *Cdhr23* or *Cdhr15*. The density of PV interneuron cell bodies in the AC of wild-type, *Cdhr23*$^{-/-}$ and *Cdhr15*$^{av\text{-}3J/av\text{-}3J}$ mice (*A*) and in the AC of *Cdhr23*$^{+/-}$ and *Cdhr15*$^{+/av\text{-}3J}$ mice with/without audiogenic seizures (AS^{+}/AS^{-} mice) on P27 (*B*) is illustrated; coronal sections (*Upper*) and detailed views (*Lower*) are shown. Note that the remaining PV interneurons in *Cdhr23*$^{-/-}$ and *Cdhr15*$^{av\text{-}3J/av\text{-}3J}$ mice, and in *Cdhr23*$^{+/-}$ and *Cdhr15*$^{+/av\text{-}3J}$ mice with audiogenic seizures, have lower density dendritic arborization than in wild-type mice. (*C*) Density of SST interneuron cell bodies in the AC of wild-type, *Cdhr23*$^{-/-}$, and *Cdhr15*$^{av\text{-}3J/av\text{-}3J}$ mice, and in the AC of *Cdhr23*$^{+/-}$ and *Cdhr15*$^{+/av\text{-}3J}$ AS^{+}/AS^{-} mice on P27; coronal sections of the AC of wild-type, *Cdhr23*$^{-/-}$, and *Cdhr15*$^{av\text{-}3J/av\text{-}3J}$ P27 mice immunostained for PV and SST are shown. Note that the SST interneuron density was not linked to a susceptibility to audiogenic seizures ($P = 0.22$). The density of PV interneuron cell bodies in the somatosensory (*D*) and motor cortices (*E*) of wild-type, *Cdhr23*$^{+/-}$, and *Cdhr15*$^{+/av\text{-}3J}$ P27 mice is illustrated; coronal sections of the wild-type mice and *Cdhr23*$^{+/-}$ mice displaying audiogenic seizures immunostained for PV and SST are shown. Data are means ± SEM, with individual values (open circles). The number of mice analyzed for each genotype is indicated between brackets. $^{**}P < 10^{-2}$, ns, not significant, nonparametric two-tailed Mann–Whitney test. AS^{+}/AS^{-} mice, mice with/without audiogenic seizures; d, dorsal; H, hippocampus; l, lateral; m, medial.

susceptibility of *Cdhr23*$^{+/-}$ and *Cdhr15*$^{+/av\text{-}3J}$ mice to audiogenic seizures, reflex seizures triggered by loud sounds (27). Audiogenic seizures were observed in a large proportion of *Cdhr23*$^{+/-}$ (51%, $n = 49$) and *Cdhr15*$^{+/av\text{-}3J}$ (38%, $n = 50$) mice, but not in their wild-type littermates ($n = 40$ and $n = 36$, respectively; $P < 10^{-4}$ for both comparisons). These seizures occurred only in mice with at least a 1.6-fold decrease in the number of PV interneurons in the AC ($P < 10^{-4}$ for both comparisons; Fig. 3*B*). This susceptibility was not linked to the sex of the affected mice (10 of 20 females and 11 of 23 males for affected *Cdhr23*$^{+/-}$ mice, $P = 0.87$; six of 20 females and 13 of 24 males for affected *Cdhr15*$^{+/av\text{-}3J}$ mice, $P = 0.19$) or to the sex of the parent transmitting the

mutation (14 of 25 and 10 of 18 offspring produced by *Cdhr23*$^{+/-}$ mothers and fathers, respectively, $P = 0.77$; six of 15 and 13 of 29 offspring produced by *Cdhr15*$^{+/av\text{-}3J}$ mothers and fathers, respectively, $P = 0.98$). In contrast, the numbers of SST interneurons were normal in the AC of *Cdhr23*$^{+/-}$ and *Cdhr15*$^{+/av\text{-}3J}$ mice ($P = 0.91$ and $P = 0.85$, respectively; Fig. 3*C*). Notably, the numbers of PV interneurons in the somatosensory and motor cortices were unaffected in *Cdhr23*$^{+/-}$ and *Cdhr15*$^{+/av\text{-}3J}$ mice ($P = 0.63$, $P = 1$ and $P = 0.11$, $P = 0.85$ in the somatosensory cortex of *Cdhr23*$^{+/-}$ and *Cdhr15*$^{+/av\text{-}3J}$ mice and in the motor cortex of *Cdhr23*$^{+/-}$ and *Cdhr15*$^{+/av\text{-}3J}$ mice, respectively; Fig. 3 *D* and *E*). Thus, the absence of cdhr23 or cdhr15 severely impairs the development of PV interneurons in the AC but not in other cortices.

Mutant Mice Deficient for *Cdhr23* or *Cdhr15* in GABAergic Interneurons Have Abnormally Small Numbers of PV Interneurons in the AC. We looked for the origin of the PV interneuron deficit in *Cdhr23*$^{-/-}$ and *Cdhr15*$^{av\text{-}3J/av\text{-}3J}$ mice. We used *Nkx2.1*-cre:*Rosa*-tdTomato mice (19) to inactivate *Cdhr23* and *Cdhr15* conditionally in MGE-derived interneuron precursors. *Nkx2.1* is transiently expressed by cortical interneuron precursors of the MGE and preoptic area, which give rise to all of the PV and SST interneurons of the neocortex (19, 28). We crossed *Nkx2.1*-cre:*Rosa*-tdTomato mice (19) with either *Cdhr23*$^{lox/lox}$ mice (29) or *Cdhr15*$^{lox/lox}$ mice to obtain *Nkx2.1*-cre:*Rosa*-tdTomato; *Cdhr23*$^{lox/lox}$ mutant mice or *Nkx2.1*-cre:*Rosa*-tdTomato; *Cdhr15*$^{lox/lox}$ mutant mice [hereafter referred to as *Cdhr23* conditional KO (cKO) or *Cdhr15* cKO mice]. *Cdhr23*$^{lox/lox}$ or *Cdhr15*$^{lox/lox}$ littermates that do not express *cre*, or *Nkx2.1*-cre:*Rosa*-tdTomato mice, were used as controls. On P27, audiogenic seizures were detected in 87% of *Cdhr23* cKO mice ($n = 18$) and 73% of *Cdhr15* cKO mice ($n = 15$), but in none of their control littermates ($P < 10^{-5}$ and $P < 10^{-3}$ for *Cdhr23* cKO and *Cdhr15* cKO mice, respectively). Markedly fewer PV interneurons were detected in the AC of P27 *Cdhr23* cKO (2.3-fold fewer; $P = 0.008$) and *Cdhr15* cKO mice (2.4-fold fewer; $P = 0.008$) than in *Nkx2.1*-cre:*Rosa*-tdTomato mice (Fig. 4 and Fig. S4). In contrast, the numbers of SST interneurons in the AC were normal in *Cdhr23* cKO ($P = 0.69$) and *Cdhr15* cKO mice ($P = 0.22$; Fig. 4). The numbers of tdTomato$^+$ interneurons, in which PV or SST was not detected, were unchanged in *Cdhr23* cKO ($P = 0.42$) and *Cdhr15* cKO mice ($P = 0.15$; Fig. 4), which excludes the possibility that a mere loss of PV expression without loss of interneurons could account for the abnormally small number of PV interneurons. This finding demonstrates that the deficit of PV interneurons in the AC results from the lack of expression of *Cdhr23* or *Cdhr15* in MGE-derived interneuron precursors.

Loss of PV Interneurons upon in Situ Deletion of *Cdhr15* in the Temporal Cortex of Newborn Mice. We then assessed the role of cdhr23 and cdhr15 at early postnatal stages by studying the impact of a postnatal in situ deletion of *Cdhr15* in the temporal cortex. A lentiviral vector encoding a cre recombinase fused to the green fluorescent protein (LV-*cre-GFP*) was injected into the temporal cortex of *Cdhr15*$^{lox/lox}$ mice on P1 (LV-*cre-GFP* P1-injected *Cdhr15*$^{lox/lox}$ mice), when immature neurons begin to form synapses (30). Cdhr15 and cdhr23 were no longer detected in the AC of these mice on P5 (Fig. 5*A*). Moreover, in these mice, but not in LV-*cre-GFP* P1-injected wild-type mice, many AC neurons stained for both GFP and the GABAergic interneuron marker Dlx5 (31) expressed, mostly in layer IV, caspase-3, a protein involved in cell apoptosis (Fig. S5*B*). On P24, audiogenic seizures were observed in all LV-*cre-GFP* P1-injected *Cdhr15*$^{lox/lox}$ mice ($n = 12$), but not in LV-*cre-GFP* P1-injected wild-type mice ($n = 7$; $P < 10^{-4}$) or other controls, including noninjected *Cdhr15*$^{lox/lox}$ mice ($n = 8$, $P < 10^{-4}$), LV-*GFP* P1-injected *Cdhr15*$^{lox/lox}$ mice ($n = 4$, $P < 10^{-3}$), and *Cdhr15*$^{lox/lox}$ mice receiving an LV-*cre-GFP* injection into the temporal cortex on P10 ($n = 8$, $P < 10^{-4}$) or into the motor cortex on P1 ($n = 9$, $P < 10^{-4}$). LV-*cre-GFP* P1-injected *Cdhr15*$^{lox/lox}$ mice that received an injection in the temporal cortex had markedly fewer PV interneurons in the AC (2.6-fold fewer) than LV-*cre-GFP* P1-injected wild-type mice ($n = 6$ for both genotypes; $P = 0.004$; Fig. 5 *B* and *C*), with unaffected auditory brainstem response thresholds (Fig. S5*A*). Thus, PV interneuron deficits restricted to the AC can cause audiogenic seizures. Moreover, these results demonstrate the crucial role of cdhr15 in the survival of immature interneurons of the AC that give rise to PV interneurons.

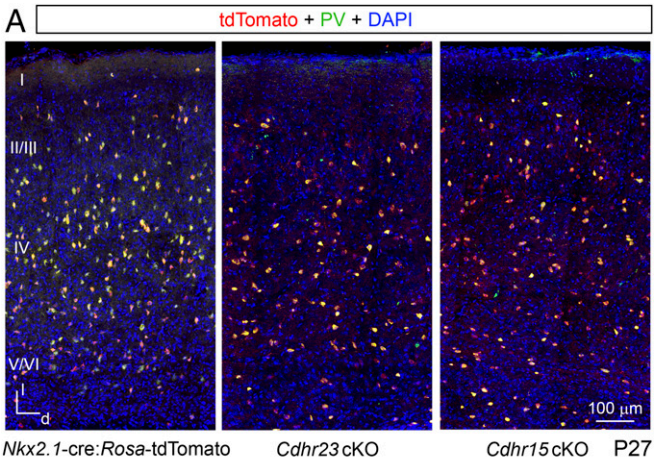

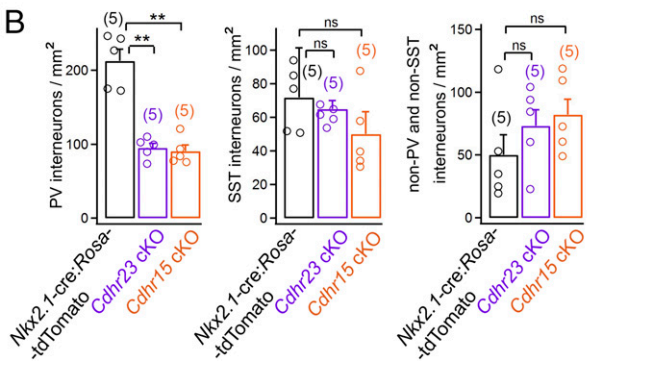

Fig. 4. Abnormally small number of PV interneurons in the AC of mice with conditional deletion of *Cdhr23* or *Cdhr15* in MGE-derived interneuron precursors. (*A*) Coronal sections of the AC of *Nkx2.1*-cre:*Rosa*-tdTomato, *Cdhr23* cKO, and *Cdhr15* cKO mice on P27 immunostained for PV and tdTomato. (*B*) Bar graphs showing the density of cell bodies of PV interneurons, SST interneurons, and tdTomato$^+$ interneurons that do not express PV or SST in the AC of *Nkx2.1*-cre:*Rosa*-tdTomato, *Cdhr23* cKO, and *Cdhr15* cKO mice on P27. Data are means ± SEM, with individual values (open circles). The number of mice analyzed for each genotype is indicated between brackets. $^{**}P < 10^{-2}$, ns, not significant, nonparametric two-tailed Mann–Whitney test. d, dorsal; l, lateral.

A Population of Interneuron Precursors Requires both Cdhr23 and Cdhr15 to Enter the Embryonic Cortex. We then investigated a possible role of cdhr23 and cdhr15 in the early development of cortical interneurons. On E14.5–E15.5, in *Nkx2.1*-cre:*Rosa*-tdTomato embryos, tdTomato$^+$ interneuron precursors expressing *Cdhr23* (cdhr23$^+$) and/or *Cdhr15* (cdhr15$^+$) were detected within the subpallium and along the superficial and deep tangential migratory routes of interneurons in the developing cortex (23) (Fig. 6*A* and Figs. S1*C* and S6*A*). In contrast to the postnatal in situ deletion of *Cdhr15* that led to the lack of expression of *Cdhr23* in the developing AC, interneuron precursors of *Cdhr23*$^{-/-}$ and *Cdhr15*$^{-/-}$ embryos each retained the expression

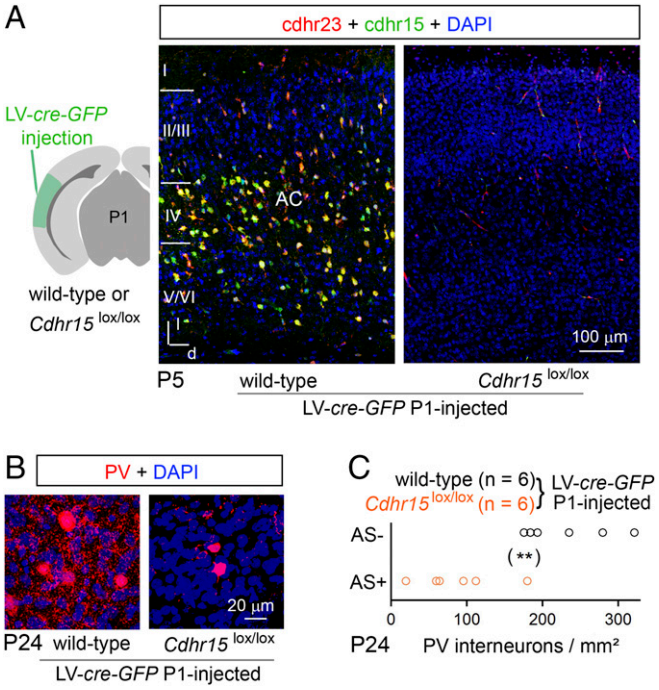

Fig. 5. In situ conditional deletion of *Cdhr15* in the AC of mice induces susceptibility to audiogenic seizures and a reduced number of PV interneurons. (*A*, *Right*) Coronal sections of the AC of wild-type and *Cdhr15*$^{lox/lox}$ P5 mice injected on P1 with the LV-*cre-GFP* recombinant virus, immunostained for cdhr23 and cdhr15. (*A*, *Left*) Site of injection is indicated in the diagram. (*B*) Detailed view of PV-immunoreactive interneurons in AC coronal sections from LV-*cre-GFP* P1-injected wild-type (*Left*) and *Cdhr15*$^{lox/lox}$ (*Right*) mice on P24. (*C*) Density of PV interneuron cell bodies in mice tested for susceptibility to audiogenic seizures. Data are individual values (open circles). $^{**}P < 10^{-2}$, nonparametric two-tailed Mann–Whitney test. d, dorsal; l, lateral.

of cdhr15 and cdhr23, respectively. Remarkably, on E14.5, cdhr15$^+$ and cdhr23$^+$ neurons in *Cdhr23*$^{-/-}$ and *Cdhr15*$^{-/-}$ embryos, respectively, were abnormally scattered throughout the subpallium (Fig. 6*B*), with no signs of apoptosis (Fig. S7*A*). They were absent from the embryonic cortex, whereas the streams of tangentially migrating neurons stained for doublecortin appeared unaffected (Fig. S7*B*). The fluorescence ratio between cdhr signals in the embryonic cortex and subpallium was much lower in *Cdhr23*$^{-/-}$ (0.07 ± 0.04, $n = 5$) and *Cdhr15*$^{-/-}$ (0.17 ± 0.05, $n = 5$) embryos than in wild-type embryos (1.2 ± 0.07, $n = 7$; $P = 0.003$ for both comparisons). Thus, both cdhr23 and cdhr15 play crucial roles in the migration of MGE-derived interneuron precursors toward the embryonic cortex.

Cell Polarity Defects in *Cdhr23*$^{-/-}$ and *Cdhr15*$^{-/-}$ MGE-Derived Interneuron Precursors. We therefore explored whether the absence of cdhr23 or cdhr15 affected the migration of MGE-derived interneuron precursors on synthetic substrates in vitro. Cdhr15$^+$ or cdhr23$^+$ neurons leaving E13.5 *Cdhr23*$^{-/-}$ or *Cdhr15*$^{-/-}$ MGE explants, respectively, cultured on a laminin substrate, migrated over much smaller areas (2.4-fold and 6.7-fold smaller, respectively) than cdhr23$^+$/cdhr15$^+$ neurons leaving wild-type MGE explants ($P < 10^{-2}$ for both comparisons; Fig. S6*B*). By contrast, the migration area was unaffected by culturing MGE explants on a cadherin-2 (cdh2, N-cadherin)/laminin substrate stimulating neurite outgrowth in vitro (32) (*Materials and Methods*; $P > 0.4$ for both comparisons; Fig. S6*C*). Both cdhr23 and cdhr15 were localized at the leading processes and growth cones (Fig. 6*C* and Fig. S6 *D* and *E*). They were coexpressed in 87% of the neurons leaving E13.5 wild-type MGE explants that express cdhr23 and/or cdhr15 ($n = 108$ neurons). The percentage of neurons with more than one process was threefold greater in cdhr15$^+$ neurons leaving *Cdhr23*$^{-/-}$ explants (18%, $n = 131$ neurons; $P = 0.004$) than in cdhr23$^+$/cdhr15$^+$ neurons leaving wild-type explants (6%, $n = 113$ neurons), but was unaffected in cdhr23$^+$ neurons leaving *Cdhr15*$^{-/-}$ explants ($n = 118$ neurons; $P = 0.74$; Fig. 6*C*). In cdhr23$^+$ neurons migrating from *Cdhr15*$^{-/-}$ explants, however, the centrosome was randomly distributed around the nucleus rather than preferentially facing the leading process as in cdhr23$^+$/cdhr15$^+$ neurons migrating from wild-type explants (Kolmogorov–Smirnov test, $P < 10^{-3}$; Fig. 6*C*) and cdhr15$^+$ neurons migrating from *Cdhr23*$^{-/-}$ explants (Kolmogorov–Smirnov test, $P = 0.95$). These cell polarity deficits of newborn interneurons are consistent with the in vivo misrouting of interneuron precursors (32) in *Cdhr23*$^{-/-}$ and *Cdhr15*$^{-/-}$ embryos (Fig. 6*B*). They suggest that both cdhr23 and cdhr15 contribute to interneuron precursor cell polarity, but through different activities.

Impaired Entry of MGE-Derived GABAergic Interneurons Expressing *Cdhr23* and *Cdhr15* into the Embryonic Cortex of Mutant Mice Lacking Adgrv1. We then asked whether the hair bundle of auditory hair cells and the interneurons of the AC share other critical proteins for their respective development. Based on the susceptibility to audiogenic seizures of *Adgrv1*$^{-/-}$ mice, which have a moderate hearing impairment on P20–P30 (33–35), we focused on adgrv1, a member of the adhesion G protein-coupled receptor family with a very long extracellular region that forms transient lateral links between stereocilia, the ankle links, during hair bundle development (36, 37) (Fig. S1 *A* and *B*). On P24, audiogenic seizures were observed in all *Adgrv1*$^{-/-}$ mice ($n = 36$), but in none of the *Adgrv1*$^{+/-}$ mice ($n = 21$; $P < 10^{-13}$). *Adgrv1*$^{-/-}$ mice also had fewer PV interneurons in the AC than their *Adgrv1*$^{+/-}$ littermates (3.1-fold fewer, $n = 5$ for both genotypes; $P = 0.008$; Fig. 7*A*), but normal numbers of AC SST interneurons ($P = 0.2$; Fig. 7*B*).

In E13.5–E14.5 mice, adgrv1 was detected in the subpallium, including the mantle zone of the MGE and the MGE ventricular zone containing MKI67-labeled progenitors (Fig. 7*C* and Fig. S8*A*). On E18.5, adgrv1 was mostly detected in the nestin-labeled processes of radial glial cells in the AC (Fig. S8*B*). In E14.5 *Adgrv1*$^{-/-}$ mice, the entry of neurons expressing cdhr23 and cdhr15 into the embryonic cortex was impaired (Fig. 7*D*). The fluorescence ratio between cdhr-immunoreactive signals in the embryonic cortex and subpallium was 34% lower in *Adgrv1*$^{-/-}$ embryos (0.8 ± 0.04, $n = 7$) than in wild-type embryos (1.2 ± 0.07, $n = 7$; $P < 10^{-3}$). Thus, adgrv1 is also involved in the development of PV interneurons in the AC, as well as in the entry of cdhr23- and cdhr15-expressing interneuron precursors into the embryonic cortex.

Similar Expression Profiles of *Cdhr23*, *Cdhr15*, and *Adgrv1* in the Mouse and Macaque. Finally, we addressed the issue of the conservation of expression profiles for cdhr23, cdhr15, and adgrv1 in primate embryos. In E63 macaque embryos [equivalent to E13–E14 mice (38)], the three proteins were immunodetected in the MGE (Fig. 8*A*). On E85 (equivalent to E17–E18 in the mouse) (38), cdhr23 and cdhr15 were detected in Dlx5-immunoreactive GABAergic interneuron precursors of the AC (31) (Fig. 8 *B* and *C* and Fig. S9) and adgrv1 was detected in the nestin-labeled processes of AC radial glial cells (Fig. 8 *B* and *D* and Fig. S9). The expression profiles of cdhr23, cdhr15, and adgrv1 in the embryonic telencephalon are thus similar in the mouse and macaque.

Discussion

Our results reveal that AC interneuron development is impaired in mutant mice defective for *Cdhr23*, *Cdhr15*, or *Adgrv1*. The lack

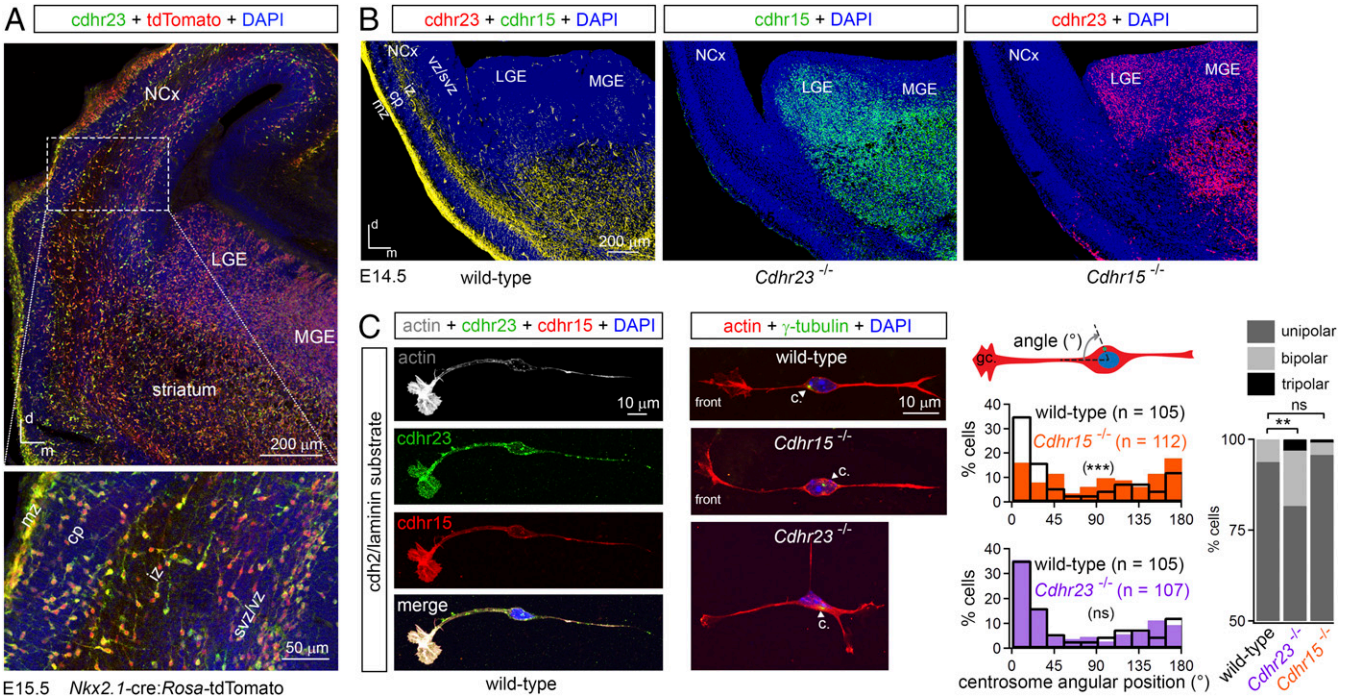

Fig. 6. Critical role of *Cdhr23* and *Cdhr15* in the migration of MGE-derived interneuron precursors. (*A*) Coronal section of the telencephalon in an *Nkx2.1*-cre:*Rosa*-tdTomato E15.5 mouse embryo immunostained for tdTomato and cdhr23 (*Upper*), and a detailed view of the neocortex (*Lower*). (*B*) Coronal sections of the telencephalon in wild-type, *Cdhr23*$^{-/-}$, and *Cdhr15*$^{-/-}$ E14.5 mouse embryos immunostained for both cdhr23 and cdhr15 (*Left*), cdhr15 (*Center*), and cdhr23 (*Right*), respectively. (*C*) Representative neurons migrating from MGE explants of a wild-type mouse, cultured on a cdh2/laminin substrate, and immunostained for actin, cdhr23, and cdhr15 without permeabilization (*Left*) or immunostained for actin and the centrosome marker γ-tubulin (arrowheads) after permeabilization (*Center*). (*Right*) Histograms show the distribution of centrosome angular positions (diagram) in unipolar cells, and the chart indicates the number of processes (one, two, or three) of cdhr15^{+} and cdhr23^{+} neurons derived from *Cdhr23*$^{-/-}$ and *Cdhr15*$^{-/-}$ MGE explants, cultured on cdh2/laminin substrate, respectively. $^{**}P < 10^{-2}$, $^{***}P < 10^{-3}$; ns, not significant, Kolmogorov–Smirnov test for the centrosome angular position data and χ^2 test for the cell polarity data. c, centrosome; cp, cortical plate; d, dorsal; gc., growth cone; iz, intermediate zone; LGE, lateral ganglionic eminence; m, medial; mz, marginal zone; NCx, neocortex; svz, subventricular zone; vz, ventricular zone.

of cdhr23, cdhr15, or adgrv1 in these mice affects the entry of *Cdhr15*-, *Cdhr23*-, and *Cdhr23*-/*Cdhr15*-expressing interneuron precursors, respectively, into the embryonic cortex, leading to a greatly decreased number of PV interneurons in the AC (Fig. S1).

The observed interneuron precursor migration deficits are not a consequence of the peripheral auditory impairment present in *Cdhr23*$^{-/-}$, *Cdhr15*$^{av\text{-}3J/av\text{-}3J}$, and *Adgrv1*$^{-/-}$ mice (12–14), because they are detectable as early as E14.5, long before the onset of hearing (~P12–P13 in mice). The abnormally small number of PV interneurons in the AC and the susceptibility to audiogenic seizures induced by the in situ deletion of *Cdhr15* in the temporal cortex on P1 revealed an additional intrinsic role of cdhr15 in the developing AC before the onset of hearing. Given the coexpression of *Cdhr23* and *Cdhr15* in immature interneurons of the AC, and the lack of expression of *Cdhr23* on P5 after the deletion of *Cdhr15*, cdhr23 probably plays a similar role in the early postnatal AC. Finally, a cortical origin for the PV interneuron deficit in the AC is further supported by the observation of a similar defect in *Cdhr23*$^{+/-}$ and *Cdhr15*$^{+/av\text{-}3J}$ mice and in *Cdhr23* cKO and *Cdhr15* cKO mice, which have no peripheral hearing deficit.

Converging lines of evidence indicate that the *Cdhr23*- and *Cdhr15*-expressing interneuron precursors of the MGE develop into PV interneurons of the AC. *Cdhr23*- and *Cdhr15*-expressing interneuron precursors are found in the ventral part of the MGE on E13.5, the time and place at which future cortical PV interneurons are generated (39). From E13.5 to P7, labeling for cdhr23 and cdhr15 is limited to MGE-derived interneuron precursors, which mature into PV and SST interneurons. By P5, *Cdhr23*- and *Cdhr15*-expressing interneuron precursors are mostly found accumulated in cortical layer IV in the AC, the preferential location of PV interneurons (40). The number of SST interneurons, the other subclass of MGE-derived interneurons, was not affected in *Cdhr23*, *Cdhr15*, and *Adgrv1* mutant mice. Moreover, *Cdhr23* and *Cdhr15* expression in interneuron precursors was found to be restricted to the developing AC on E18.5, like the decrease in the number of PV interneurons in 3-wk-old *Cdhr23* and *Cdhr15* mutant mice. Finally, the conditional deletion of *Cdhr23* and *Cdhr15* in MGE-derived interneurons at the progenitor stage reproduced the PV interneuron deficit and led to a susceptibility to audiogenic seizures. Together, these results demonstrate that the population of *Cdhr23*- and *Cdhr15*-expressing interneuron precursors of the MGE gives rise to a large fraction of the PV interneurons in the AC.

The numbers of PV interneurons in the AC of *Cdhr23*$^{+/-}$ and *Cdhr15*$^{+/av\text{-}3J}$ mice, although systematically small, differed strongly between individual mice, as did susceptibility to audiogenic seizures. The origin of this heterogeneity remains unclear, but it was not related to the sex of the affected heterozygous mouse or of the parent transmitting the mutation (which would have suggested genomic imprinting of *Cdhr23* and *Cdhr15*). Genetic background or a random monoallelic expression of *Cdhr23* and *Cdhr15* in the telencephalon [already reported for both genes in neural progenitor cells derived from mouse ES cells (41)] may account for this variability.

What roles do cdhr23 and cdhr15 play in interneuron precursors? Migration areas were markedly smaller for cdhr15^{+} interneuron precursors and cdhr23^{+} interneuron precursors growing out of *Cdhr23*$^{-/-}$ and *Cdhr15*$^{-/-}$ MGE explants cultured on laminin substrate, respectively, than for cdhr23^{+}/cdhr15^{+} interneuron precursors growing out of wild-type MGE explants,

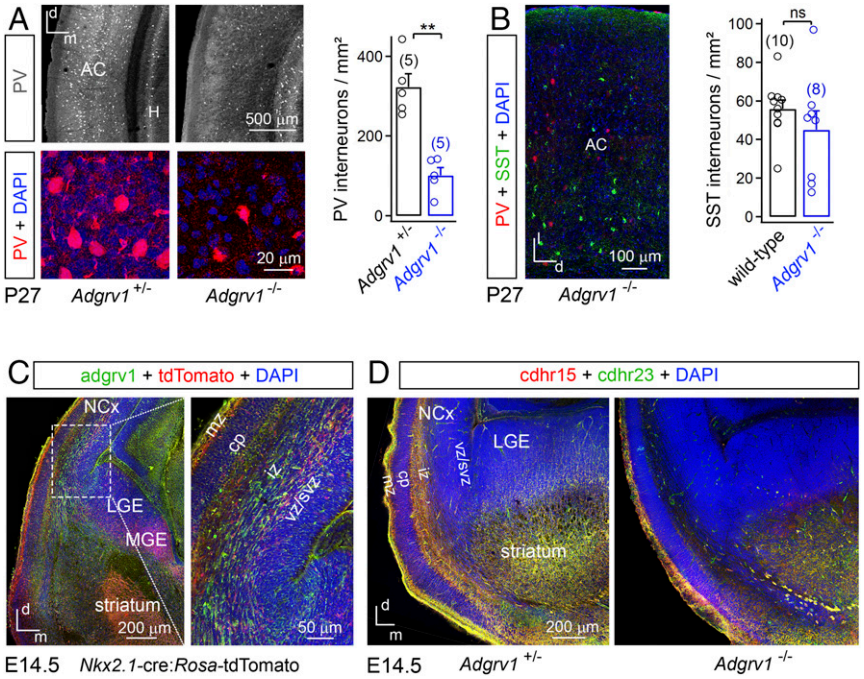

Fig. 7. Defective development of MGE-derived cdhr23^{+}/cdhr15^{+} GABAergic interneurons in *Adgrv1*$^{-/-}$ mice. (*A*) Coronal sections of the AC of *Adgrv1*$^{+/-}$ and *Adgrv1*$^{-/-}$ P27 mice immunostained for PV (*Upper*) with detailed views (*Lower*), and a bar graph showing the density of PV interneuron cell bodies. (*B*) Coronal section of the AC of an *Adgrv1*$^{-/-}$ P27 mouse immunostained for PV and SST, and a bar graph showing the density of SST interneuron cell bodies in wild-type and *Adgrv1*$^{-/-}$ mice. (*C*) Coronal sections of the telencephalon of an *Nkx2.1*-cre:*Rosa*-tdTomato mouse embryo on E14.5 immunostained for tdTomato and adgrv1 (*Left*), and a detailed view of the embryonic cortex (*Right*). (*D*) Coronal sections of the telencephalon of *Adgrv1*$^{+/-}$ (*Left*) and *Adgrv1*$^{-/-}$ (*Right*) mouse embryos on E14.5 immunostained for cdhr23 and cdhr15. Data are means ± SEM with individual values (open circles). $^{**}P < 10^{-2}$, ns, not significant, nonparametric two-tailed Mann–Whitney test. The number of mice analyzed for each genotype is indicated between brackets. cp, cortical plate; d, dorsal; H, hippocampus; iz, intermediate zone; l, lateral; LGE, lateral ganglionic eminence; m, medial; mz, marginal zone; NCx, neocortex; svz, subventricular zone; vz, ventricular zone.

suggesting a motility deficit and/or a polarity defect of these migrating neurons. The migration areas observed on a substrate consisting of cdh2 and laminin, promoting the motility of interneuron precursors, were no smaller than normal, but neurons lacking either cdhr23 or cdhr15 displayed cell polarity defects, albeit with different manifestations. These cell polarity defects are consistent with the dispersion of these interneuron precursors in the subpallium of mutant embryos. On P1, a developmental time point at which interneuron precursors have reached their final AC destination, the in situ deletion of *Cdhr15* in the temporal cortex led to apoptosis of local interneuron precursors. This additional role of cdhr15 may reflect the early involvement of this cdhr in GABAergic interneuron synaptogenesis, which is considered to be essential for interneuron survival (42). This dual role is reminiscent of the role reported for two other adhesion proteins in GABAergic interneuron precursors in the embryonic telencephalon: celsr3 (also known as adgrc3) (43) [from the flamingo cadherin (9) and adhesion G protein-coupled receptor families (44)] and cdh2 (32). However, these two proteins are not required for the specific targeting of interneuron precursors to a particular neocortical area. Cdh2 is critically involved in the cell polarity and migration of GABAergic interneuron precursors, whereas celsr3 is required for the entry of interneuron precursors expressing calbindin-2 (also known as calretinin) into the embryonic cortex, and both proteins are also involved in synaptogenesis (45, 46).

Previous studies have shown that most clonally related interneurons derived from the MGE are targeted to one telencephalon structure (47–49), where they form clusters (50, 51). Regardless of the possible clonal relationship between *Cdhr23*- and *Cdhr15*-expressing GABAergic interneuron precursors in the AC, our results indicate that these precursors are targeted specifically to the AC immediately after their birth. Based on the critical role of adhesion proteins cdhr23 and cdhr15 in the targeting and survival of newly born GABAergic interneuron precursors in a specific cortical area (the developing AC) reported here, we suggest that there is an "adhesion code" that functions early in development and targets particular populations of newborn MGE-derived GABAergic interneuron precursors to functionally specific areas of the neocortex.

The conservation, from the mouse to macaque, of the expression profiles of the three proteins studied here suggests the existence of an intrinsic deficit of PV interneurons in the AC of humans carrying *CDHR23*, *CDHR15*, or *ADGRV1* mutations, despite differences in the origin of these neurons in the human brain (52). After the fitting of cochlear implants, some of these patients have been reported to face unusual speech-recognition difficulties not observed in patients with mutations of other deafness genes (53). These difficulties might be related to the involvement of PV interneurons in the experience-driven neural plasticity underlying AC maturation (8, 54) and the temporal precision of sound detection critical for speech perception (55). The shaping of the perception of several acoustic features throughout life, including frequency discrimination acuity (56) and the detection of unexpected sounds, also involves PV interneurons of the AC (57).

The results presented here suggest the possible involvement of other deafness genes underlying peripheral auditory deficits in the development and functioning of the AC. Mutations of *CDHR23* or *CDHR15* and of *ADGRV1* are responsible for type 1 and type 2 Usher syndrome, respectively. These autosomal recessive disorders combine congenital hearing impairment with delayed-onset sight loss. The formation of protein complexes containing cdhr23, cdhr15, or adgrv1, together with other Usher syndrome gene products, in both hair cells and photoreceptor cells (58–60) identifies these proteins as attractive candidates for

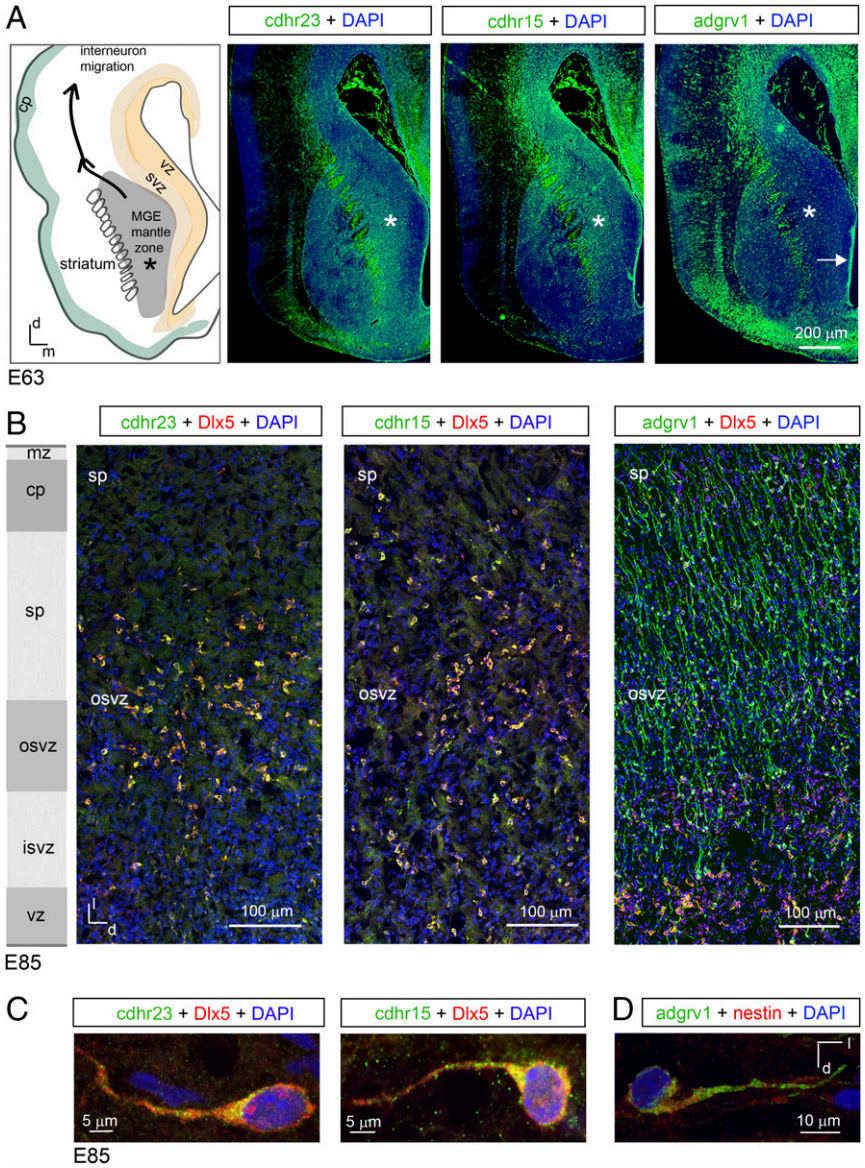

Fig. 8. Expression of *Cdhr23*, *Cdhr15*, and *Adgrv1* in the MGE and developing AC of macaque embryos. (*A*) Coronal sections of the telencephalon in an E63 macaque embryo immunostained for cdhr23, cdhr15, or adgrv1. The MGE mantle zone is indicated by an asterisk, and the MGE ventricular zone is indicated by an arrow. The different regions are shown on the diagram. (*B*) Sagittal sections of the developing AC of an E85 macaque embryo immunostained for Dlx5 and cdhr23, cdhr15, or adgrv1 showing the outer subventricular zone and the subplate (diagram of the brain cortical layers on the left side). High-magnification views of GABAergic interneuron precursors in the outer subventricular zone immunostained for Dlx5 and either cdhr23 or cdhr15 (*C*) and of a radial glial cell immunostained for adgrv1 and nestin, a radial glia marker (*D*), are shown. cp, cortical plate; d, dorsal; isvz, inner subventricular zone; l, lateral; m, medial; osvz, outer subventricular zone; sp, subplate svz, subventricular zone; vz, ventricular zone.

involvement in AC interneuron development. Broadening our view by identifying the other proteins involved will help to clarify the evolutionary steps accounting for the use of the same essential proteins for the development of the cochlea and the AC.

The impact of sensory deprivation on AC development in people with genetic forms of deafness has so far overshadowed the consideration of possible intrinsic cortical deficiencies. Advances in our understanding of the hidden intrinsic cortical deficits of hereditary forms of deafness should provide a scientific basis for improving auditory rehabilitation in patients and for the development of cortical therapies. This work should also pave the way for the development of a genetic approach to the cellular and molecular mechanisms involved in AC development and functioning.

Materials and Methods

A detailed description of the methods is available in *SI Materials and Methods*. Animal experiments were carried out in accordance with French and European regulations. Approval for the experiments using animals was obtained from the Animal Use Committee of the Institut Pasteur. Susceptibility to audiogenic seizures was evaluated using high-intensity (100–110 dB) continuous pure tones (8–15 kHz) lasting up to 1 min. Hearing tests were performed as described by Møller and Jannetta (61) and Avan et al. (62). For immunofluorescence analyses, the antibodies directed against cdhr23 and cdhr15 were used as described by Pepermans et al. (16) and Sahly et al. (59). Culture of MGE explants and quantification of neuronal migration were carried out as described by Luccardini et al. (32).

ACKNOWLEDGMENTS. We thank M. Bosch Grau, S. Chardenoux, A. Emptoz, C. Leclech, D. Oficjalska, M. Pedraza Boti, E. Pepermans, C. Trébeau, and D. Weil for assistance with this project; and J.-P. Hardelin for his important

contribution to the writing of the manuscript. We thank S. Etienne-Manneville (Institut Pasteur, Paris) and S. Garel (Ecole Normale Supérieure, Paris) for advice. We thank G. Lepousez (Institut Pasteur, Paris) and N. Renier (Institut du Cerveau et de la Moelle Epinière, Paris) for critical reading of the manuscript. We thank C. Dehay (PrimaLyon Platform, Institut Cellule Souche et Cerveau, INSERM, Bron, France), N. Kessaris (University College London, London), and M. Sato (University of Fukui, Fukui, Japan) for sharing brain sections from macaque embryos, *Nkx2.1*-cre:*Rosa*-tdTomato mice, and *Adgrv1*^{tm1Msat} mice, respectively. We acknowledge the Imagopole/Citech facility (Institut Pasteur, Paris), which is part of the France BioImaging infrastructure supported by the French Agence Nationale pour la Recherche (ANR-10-INSB-04-01, *Investissements d'Avenir* program), for the use of its microscopes. This work was supported by PhD funding from the French Ministry of Research allocated by the Ecole Normale Supérieure (Paris) (to B.L.-P.), the *Prix Emergence* and the SEIZEAR grant of the *Agir Pour l'Audition* foundation (to N.M.), and by grants from the ANR as part of the second *Investissements d'Avenir* program LIGHT4DEAF (ANR-15-RHUS-0001) and LabEx LIFESENSES (ANR-10-LABX-65), the European Research Council (ERC-2011-ADG_294570 to C.P.), BNP Paribas Foundation, FAUN-Stiftung, and LHW-Stiftung.

1. Petit C (1996) Genes responsible for human hereditary deafness: Symphony of a thousand. *Nat Genet* 14:385–391.
2. Richardson GP, de Monvel JB, Petit C (2011) How the genetics of deafness illuminates auditory physiology. *Annu Rev Physiol* 73:311–334.
3. Zhang LI, Bao S, Merzenich MM (2001) Persistent and specific influences of early acoustic environments on primary auditory cortex. *Nat Neurosci* 4:1123–1130.
4. Dorrn AL, Yuan K, Barker AJ, Schreiner CE, Froemke RC (2010) Developmental sensory experience balances cortical excitation and inhibition. *Nature* 465:932–936.
5. de Villers-Sidani E, Merzenich MM (2011) Lifelong plasticity in the rat auditory cortex: Basic mechanisms and role of sensory experience. *Prog Brain Res* 191:119–131.
6. Sanes DH, Bao S (2009) Tuning up the developing auditory CNS. *Curr Opin Neurobiol* 19:188–199.
7. Klinke R, Kral A, Heid S, Tillein J, Hartmann R (1999) Recruitment of the auditory cortex in congenitally deaf cats by long-term cochlear electrostimulation. *Science* 285: 1729–1733.
8. Kral A, Kronenberger WG, Pisoni DB, O'Donoghue GM (2016) Neurocognitive factors in sensory restoration of early deafness: A connectome model. *Lancet Neurol* 15: 610–621.
9. Hulpiau P, Gul IS, van Roy F (2013) New insights into the evolution of metazoan cadherins and catenins. *Prog Mol Biol Transl Sci* 116:71–94.
10. Hulpiau P, van Roy F (2009) Molecular evolution of the cadherin superfamily. *Int J Biochem Cell Biol* 41:349–369.
11. Sotomayor M, Weihofen WA, Gaudet R, Corey DP (2012) Structure of a force-conveying cadherin bond essential for inner-ear mechanotransduction. *Nature* 492:128–132.
12. Kazmierczak P, et al. (2007) Cadherin 23 and protocadherin 15 interact to form tip-link filaments in sensory hair cells. *Nature* 449:87–91.
13. Lefèvre G, et al. (2008) A core cochlear phenotype in USH1 mouse mutants implicates fibrous links of the hair bundle in its cohesion, orientation and differential growth. *Development* 135:1427–1437.
14. Petit C, Richardson GP (2009) Linking genes underlying deafness to hair-bundle development and function. *Nat Neurosci* 12:703–710.
15. Goodyear RJ, Forge A, Legan PK, Richardson GP (2010) Asymmetric distribution of cadherin 23 and protocadherin 15 in the kinocilial links of avian sensory hair cells. *J Comp Neurol* 518:4288–4297.
16. Pepermans E, et al. (2014) The CD2 isoform of protocadherin-15 is an essential component of the tip-link complex in mature auditory hair cells. *EMBO Mol Med* 6: 984–992.
17. Defelipe J (2011) The evolution of the brain, the human nature of cortical circuits, and intellectual creativity. *Front Neuroanat* 5:29.
18. Markram H, et al. (2004) Interneurons of the neocortical inhibitory system. *Nat Rev Neurosci* 5:793–807.
19. Kessaris N, et al. (2006) Competing waves of oligodendrocytes in the forebrain and postnatal elimination of an embryonic lineage. *Nat Neurosci* 9:173–179.
20. Marín O, Müller U (2014) Lineage origins of GABAergic versus glutamatergic neurons in the neocortex. *Curr Opin Neurobiol* 26:132–141.
21. Faux C, Rakic S, Andrews W, Britto JM (2012) Neurons on the move: Migration and lamination of cortical interneurons. *Neurosignals* 20:168–189.
22. Rudy B, Fishell G, Lee S, Hjerling-Leffler J (2011) Three groups of interneurons account for nearly 100% of neocortical GABAergic neurons. *Dev Neurobiol* 71:45–61.
23. Marín O (2013) Cellular and molecular mechanisms controlling the migration of neocortical interneurons. *Eur J Neurosci* 38:2019–2029.
24. Xu Q, Cobos I, De La Cruz E, Rubenstein JL, Anderson SA (2004) Origins of cortical interneuron subtypes. *J Neurosci* 24:2612–2622.
25. Zheng QY, et al. (2005) Digenic inheritance of deafness caused by mutations in genes encoding cadherin 23 and protocadherin 15 in mice and humans. *Hum Mol Genet* 14: 103–111.
26. Houser CR (2014) Do structural changes in GABA neurons give rise to the epileptic state? *Adv Exp Med Biol* 813:151–160.
27. Italiano D, et al. (2016) Genetics of reflex seizures and epilepsies in humans and animals. *Epilepsy Res* 121:47–54.
28. Nóbrega-Pereira S, et al. (2008) Postmitotic Nkx2-1 controls the migration of telencephalic interneurons by direct repression of guidance receptors. *Neuron* 59:733–745.
29. Etournay R, et al. (2010) Cochlear outer hair cells undergo an apical circumference remodeling constrained by the hair bundle shape. *Development* 137:1373–1383.
30. Le Magueresse C, Monyer H (2013) GABAergic interneurons shape the functional maturation of the cortex. *Neuron* 77:388–405.
31. Eisenstat DD, et al. (1999) DLX-1, DLX-2, and DLX-5 expression define distinct stages of basal forebrain differentiation. *J Comp Neurol* 414:217–237.
32. Luccardini C, et al. (2013) N-cadherin sustains motility and polarity of future cortical interneurons during tangential migration. *J Neurosci* 33:18149–18160.
33. Frings H, Frings M (1951) Otitis media and audiogenic seizures in mice. *Science* 113: 689–690.
34. Yagi H, et al. (2005) Vlgr1 knockout mice show audiogenic seizure susceptibility. *J Neurochem* 92:191–202.
35. Skradski SL, et al. (2001) A novel gene causing a mendelian audiogenic mouse epilepsy. *Neuron* 31:537–544.
36. McGee J, et al. (2006) The very large G-protein-coupled receptor VLGR1: A component of the ankle link complex required for the normal development of auditory hair bundles. *J Neurosci* 26:6543–6553.
37. Michalski N, et al. (2007) Molecular characterization of the ankle-link complex in cochlear hair cells and its role in the hair bundle functioning. *J Neurosci* 27: 6478–6488.
38. Dehay C, Kennedy H (2007) Cell-cycle control and cortical development. *Nat Rev Neurosci* 8:438–450.
39. Sultan KT, Brown KN, Shi SH (2013) Production and organization of neocortical interneurons. *Front Cell Neurosci* 7:221.
40. Tremblay R, Lee S, Rudy B (2016) GABAergic interneurons in the neocortex: From cellular properties to circuits. *Neuron* 91:260–292.
41. Gendrel AV, et al. (2014) Developmental dynamics and disease potential of random monoallelic gene expression. *Dev Cell* 28:366–380.
42. Bartolini G, Ciceri G, Marín O (2013) Integration of GABAergic interneurons into cortical cell assemblies: Lessons from embryos and adults. *Neuron* 79:849–864.
43. Ying G, et al. (2009) The protocadherin gene Celsr3 is required for interneuron migration in the mouse forebrain. *Mol Cell Biol* 29:3045–3061.
44. Hamann J, et al. (2015) International Union of Basic and Clinical Pharmacology. XCIV. Adhesion G protein-coupled receptors. *Pharmacol Rev* 67:338–367.
45. Arikkath J, Reichardt LF (2008) Cadherins and catenins at synapses: Roles in synaptogenesis and synaptic plasticity. *Trends Neurosci* 31:487–494.
46. Thakar S, et al. (2017) Evidence for opposing roles of Celsr3 and Vangl2 in glutamatergic synapse formation. *Proc Natl Acad Sci USA* 114:E610–E618.
47. Mayer C, et al. (2015) Clonally related forebrain interneurons disperse broadly across both functional areas and structural boundaries. *Neuron* 87:989–998.
48. Harwell CC, et al. (2015) Wide dispersion and diversity of clonally related inhibitory interneurons. *Neuron* 87:999–1007.
49. Sultan KT, et al. (2016) Clonally related GABAergic interneurons do not randomly disperse but frequently form local clusters in the forebrain. *Neuron* 92:31–44.
50. Brown KN, et al. (2011) Clonal production and organization of inhibitory interneurons in the neocortex. *Science* 334:480–486.
51. Ciceri G, et al. (2013) Lineage-specific laminar organization of cortical GABAergic interneurons. *Nat Neurosci* 16:1199–1210.
52. Geschwind DH, Rakic P (2013) Cortical evolution: Judge the brain by its cover. *Neuron* 80:633–647.
53. Wu CC, et al. (2015) Identifying children with poor cochlear implantation outcomes using massively parallel sequencing. *Medicine (Baltimore)* 94:e1073.
54. Kral A, Tillein J, Heid S, Klinke R, Hartmann R (2006) Cochlear implants: Cortical plasticity in congenital deprivation. *Prog Brain Res* 157:283–313.
55. Weible AP, et al. (2014) Perceptual gap detection is mediated by gap termination responses in auditory cortex. *Curr Biol* 24:1447–1455.
56. Aizenberg M, Mwilambwe-Tshilobo L, Briguglio JJ, Natan RG, Geffen MN (2015) Bidirectional regulation of innate and learned behaviors that rely on frequency discrimination by cortical inhibitory neurons. *PLoS Biol* 13:e1002308.
57. Natan RG, et al. (2015) Complementary control of sensory adaptation by two types of cortical interneurons. *Elife* 4:e9868.
58. Michalski N, Petit C (2015) Genetics of auditory mechano-electrical transduction. *Pflugers Arch* 467:49–72.
59. Sahly I, et al. (2012) Localization of Usher 1 proteins to the photoreceptor calyceal processes, which are absent from mice. *J Cell Biol* 199:381–399.
60. Schietroma C, et al. (2017) Usher syndrome type 1-associated cadherins shape the photoreceptor outer segment. *J Cell Biol* 216:1849–1864.
61. Møller AR, Jannetta PJ (1983) Interpretation of brainstem auditory evoked potentials: Results from intracranial recordings in humans. *Scand Audiol* 12:125–133.
62. Avan P, Büki B, Petit C (2013) Auditory distortions: Origins and functions. *Physiol Rev* 93:1563–1619.
63. Yagi H, et al. (2007) Vlgr1 is required for proper stereocilia maturation of cochlear hair cells. *Genes Cells* 12:235–250.
64. Lallemand Y, Luria V, Haffner-Krausz R, Lonai P (1998) Maternally expressed PGK-Cre transgene as a tool for early and uniform activation of the Cre site-specific recombinase. *Transgenic Res* 7:105–112.
65. Ross KC, Coleman JR (2000) Developmental and genetic audiogenic seizure models: Behavior and biological substrates. *Neurosci Biobehav Rev* 24:639–653.
66. Gavrieli Y, Sherman Y, Ben-Sasson SA (1992) Identification of programmed cell death in situ via specific labeling of nuclear DNA fragmentation. *J Cell Biol* 119:493–501.
67. Paxinos G, Franklin KBJ (2001) *The Mouse Brain in Stereotaxic Coordinates* (Academic, San Diego), 2nd Ed.